Mapana – Journal of Sciences
2024, Vol. 23, No. 4, 1-27
ISSN 0975-3303 | https://doi.org/10.12723/mjs.71.1

A Mini-Review on Laser-Produced Plasma in an External Magnetic Field: Plasma Confinement and Optical Emission Enhancement

Khwairakpam Shantakumar Singh*

Abstract

The present work aims to provide an overview of magnetic-assisted ablation and subsequent production of plasma by laser. The paper discusses physical phenomena involved in magnetic field-assisted ablation, such as laser ablation efficiency enhancement, improvement in optical emission, plasma plume confinement, instability, and so on. It systematically reviews the studies conducted in the previous seven years on the effect of magnetic field on material removal using laser, which will help researchers assess current challenges and uses of magnetised laser plasma. It describes experimental techniques such as optical emission spectroscopy and imaging. This paper aims to help researchers investigating laser plasmas understand the fundamentals of magnetic field-assisted laser ablation, specifically focusing on physical phenomena, major challenges, methodologies, and applications.

Keywords: Laser ablation, magnetic confinement, enhancement of optical emission

1. Introduction

Focusing a high-power laser on any type of material, such as gases, liquids, solids, aerosols, etc., generates laser-produced plasma (LPP). [1]. Laser-induced heating triggers melting, vaporisation, plasma

* Department of Education, Assam University Silchar, Assam - 788011, India; khwairakpam.shantakumar@aus.ac.in; shantakh9@gmail.com, ORCID ID 0000-0003-4745-8388

generation, plasma expansion, and particle generation. Fundamental and applied studies have focused on magnetised LPP in recent years. Putting LPP in a magnetic field causes a lot of interesting things to happen, such as the confinement of a plasma plume [2–4], optical emission enhancement [5–14], instability [15], ion acceleration [16], adiabatic compression, Joule's heating, enhancement of ablation rate, and more. For various reasons, researchers have extensively investigated magnetic field-assisted ablation of matter by laser and subsequent LPP dynamics using experimental and numerical methods [16–26]. The magnetic field-assisted laser ablation (LA) enhances the mass removal rate of various types of material. Farrokhi et al. [26] looked at how a magnetic field (0.192 T) affected the removal of Si material using the UV nanosecond laser. They discovered an increase in the depth of the crater by 1.3-69 times. The depth enhancement is due to magneto-absorption effects. In the provided reference [20,26–32], we find additional research on the laser ablation magnetic field. Some of them claim that increasing plasma-target heat flow is the way to increase the ablation rate [17,33–35]. Researchers use laser-induced breakdown spectroscopy (LIBS) for sample composition analysis. Various fields have employed LIBS, including remote elemental analysis, artwork diagnostics, online alloy analysis in industries, radioactive element detection, and soil analysis [1]. This spectroscopic technique used the emission of LPP. The material composition of the sample is analysed by recording the spectra emitted from the LPP. There are many advantages to LIBS. For example, any type of sample, such as gases, aerosols, liquids, and solids, can undergo analysis using LIBS. LIBS allows for simultaneous multielement analysis and in situ measurements, requiring no preparation of sample or relatively simple preparation. Despite the aforementioned advantages, its low sensitivity remains a significant issue, prompting many research groups to investigate and design various techniques to increase plasma emissions. They used a number of methods for enhancing the intensity of the LPP emission, including removing the surrounding gas[36], using double pulse excitation [7,37–41], oblique laser incidence [11], an external magnetic field [5,6,11,14,36,42–46], and spatial confinement [9,47]. Recently, studies on magnetised LPP have significantly increased, as this technique enhances the optical emission intensity. The study

examines the previous research on optical emission enhancement in magnetically confined LPP and its current trend. The paper discusses, analyses and presents the physical phenomena associated with the magnetised LPP. This review also highlights the potential applications of magnetised LPP. The literature survey on magnetically confined plasma was conducted systematically, and the pie chart in Figure 1 shows the percentage distribution of some reports on magnetically confined plasma documented in the last few years. This suggests a substantial increase in magnetised LPP studies over the last five to six years, which continues to this day. Recently, the LIBS signal enhancement by the application of a magnetic field was observed by Li et al. and Khan et al. [48–50]

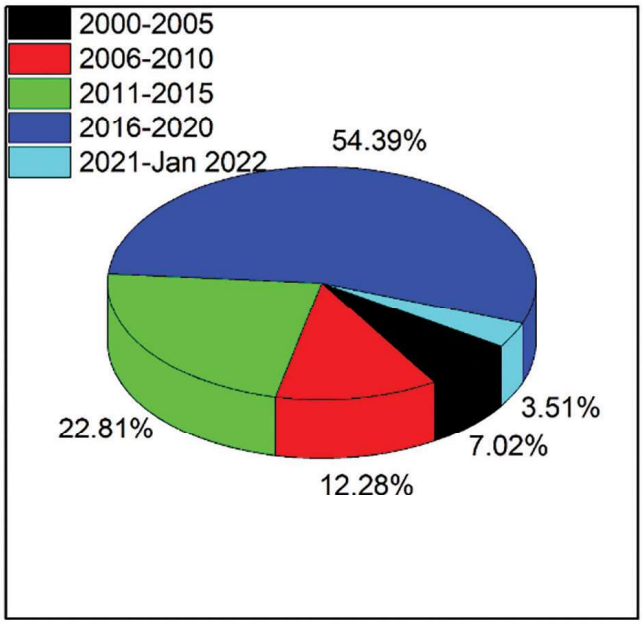

Fig.1. Percentage distribution of available reports in the literature in recent years.

However, there is still a considerable lack of understanding of these phenomena. Consequently, the interest in exploiting LPP in the magnetic field is growing. This review focuses mainly on plasma plume confinement and optical emission enhancement. The paper discusses LA, confinement of LPP plume, instability, and emission enhancement. It also describes the optical emission spectroscopy (OES) and imaging techniques used to study LPP. The last part of

the article concludes the overall review. The documentation of comparative studies of LPP with and without magnetic fields is inadequate. This paper will help researchers understand magnetised LPP's physical processes, issues, analysis methods, and applications. Additionally, Table 1 lists some of the recent studies on magnetised LPP, along with their references, to help researchers understand the current trends in this research topic.

i. Optical Emission Spectroscopy and Imaging Technique

Various methods have been adopted to investigate LPP in an external magnetic field. Some important methods are optical emission spectroscopy[51], imaging method[2], Langmuir probe[13,52], etc. It is one of the versatile techniques for studying LPP. When a pulsed laser, such as a nanosecond laser, interacts with a metallic target, free electrons of the metal absorb the laser pulse energy through inverse Bremsstrahlung absorption. Both the electron-electron collision and the electron-atom collision cause thermalisation [1]. If the sample temperature surpasses the vaporisation temperature, the laser-focused area of the sample undergoes ablation. The ablated mass undergoes more ionisation upon further laser absorption, eventually becoming LPP. The LPP expands and interacts with the surrounding medium viz gas or liquid [14]. Within the pulse duration, the LPP expansion is isothermal. The isothermal expansion changes to an adiabatic process when the pulse ends [2], resulting in a reduction in plasma density and temperature. At a later delay time of plasma expansion, the plasma emits spectral lines. It is due to atomic or ionic transitions from a higher energy level to a lower one, as well as electron-ion recombination [1]. These spectral lines represent the characteristics of the sample's components [53,54]. The optical emission spectroscopic technique can collect and analyse the radiation emitted by LPP. A typical experimental setup of OES is shown in Figure 2.

Table 1. List of studies on magnetic field-assisted laser ablation of various materials

Year	Objectives	Reference
2021	Preparation of photodetector by laser ablation in water in the magnetic field.	Mohsin et al.[19]
2020	Effect of magnetic field on laser-plasma plume and optical emission.	Wu et al. [55]
2020	Lateral interaction of plasma plumes in a magnetic field.	Mondal et al. [56]
2019	Enhancement of LIBS signal of lead plasma by the magnetic field.	Akhtar et al. [8]
2019	Laser fabrication of bioelectrode with surface microstructure in the presence of the magnetic field.	Zhou et al. [57]
2019	Nanosecond laser ablation enhancement by the axial magnetic field and its associated fundamental mechanisms.	Farrokhi et al. [27]
2018	Studies on LPP parameters and surface characterisation of the laser-ablated copper alloy.	Dawood et al. [58]
2017	Effect of magnetic field on laser ablation and LIBS of copper plasma. Surface structuring of laser irradiated copper sample in the presence of the magnetic field.	Singh et al. [4,10,21,23,32]
2017	Magnetic confinement of LPP by applying a multicusp magnetic field.	Takahashiet al. [16]
2016	The growth of LPP in time and space in the externally applied magnetic field. Magnetic field-assisted laser ablation at different values of the magnetic field. Effect of lens-sample distance on LPP in the presence of the magnetic field.	Singh et al. [4,51,59]
2016	Magnetic field-assisted laser ablation products and LIBS. Enhancement of optical emission intensity by the magnetic field-assisted double pulse excitation.	Musaev et al., Arshad et al., and Hussain et al. [7,24,60]
2015	Effect of pulse width and magnetic field on LPP of Cu. Dynamics of laser ablation in liquid with a magnetic field.	Pandey et al. and Kim et al. [20,22]

A suitable pump, such as a rotary pump, turbomolecular pump, diffusion pump, etc., connects to the vacuum chamber to evacuate it to low pressure. We maintain the air or ambient gas pressure of the chamber according to the study's requirements. A high-power laser from a source, such as a Nd: YAG Q-switched laser source, focuses on a sample within the vacuum chamber to create plasma. Many research groups used the typical setup to study the LPP dynamics without and with a magnetic field at different ambient conditions [3–5,9,10,14,60–63]. Figure 3 depicts the arrangement of bar magnets to introduce a magnetic field to the LPP. The sample, to be ablated, is mounted in the gap between the poles of an electromagnet or permanent magnet to allow the LPP expansion in the magnetic field. The chamber accommodates this whole arrangement. A suitable translation stage is always employed to reduce sample deterioration. A spectrometer (with an ICCD detector) coupled with an optical fibre (OF) may be used to record the atomic and ionic lines of LPP at different locations of LPP. Using time-resolved optical emission spectroscopy, we can record and analyse the spectra of LPP systematically at different delay times with respect to the laser pulse.

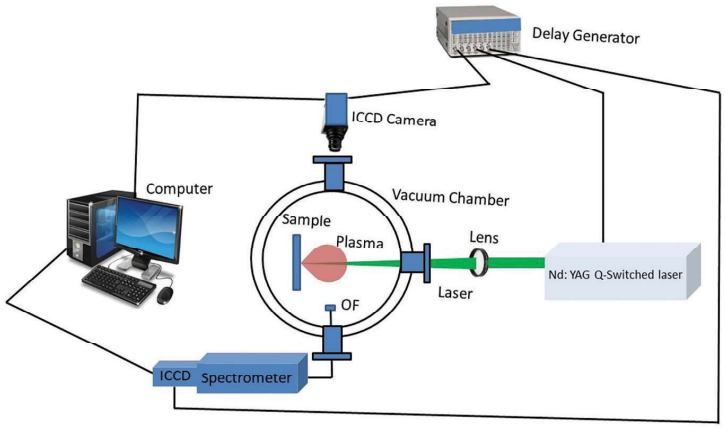

Fig.2. A typical experimental setup for imaging of LPP and time-integrated optical emission spectroscopy.

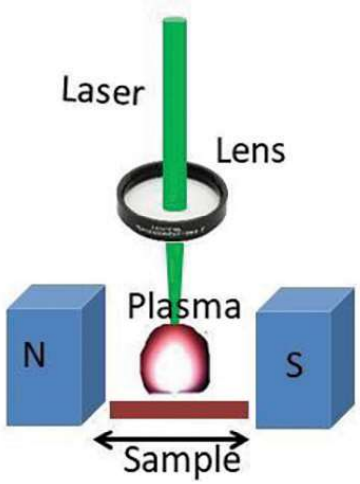

Fig. 3. Arrangement of the bar magnet and generation of plasma between two magnetic poles.

To analyse the time-integrated spectra at different times after the plasma ignition, we can use LIBS software [64]. These spectra show quantitative and qualitative information about the compositions of a sample. One can calculate the density of electrons of LPP under the local thermodynamic equilibrium (LTE) using the FWHM of the Stark profile of the atomic line. We widely employ the Boltzmann plot, which uses the atomic lines, to estimate the electron temperature of LPP [65]. By displacing the OF using a suitable translating stage, we can record the LPP spectra along the axial and lateral directions. This is known as spatially-resolved optical emission spectroscopy. An ICCD camera can also utilise the same setup to image the plasma at different times with respect to the pulse. The plasma plume dynamics are examined from the images recorded at different delay times [66]. Figure 4 shows a typical setup to explore the evolution of LPP with time. Singh et al. and other researchers employed such an experimental setup[51,59,67]. The monochromator (with a photomultiplier tube) and an OF collect plasma radiation. They record the changes in time of a certain type of plasma particle (atom or ion) using an oscilloscope that is set off by a laser signal going through a photodiode (PD) [59]. Table 2 presents several significant relationships commonly utilised to characterise plasma.

2. LPP in a Magnetic Field

We can utilise an external magnetic field to amplify the signal of LIBS. From the introduction, we understand that LPP in a magnetic field is associated with many complex phenomena. The phenomena discussed in the present article are the laser ablation process, plasma plume confinement, optical emission enhancement, and instability.

i. Laser Ablation Process

The formation of LPP begins with laser ablation. The laser ablation mechanisms of nanosecond and femtosecond lasers fall into different regimes. This review examines the mechanisms of nanosecond laser ablation, highlighting its widespread use in various industries. The main material removal processes of nanosecond lasers are vaporisation and mechanical processes (melt ejection, instability, etc.). A nanosecond laser irradiates a sample, heating its surface. The heat generated within the time of pulse width diffuses into the sample and confines itself to a depth equivalent to the diffusion length.

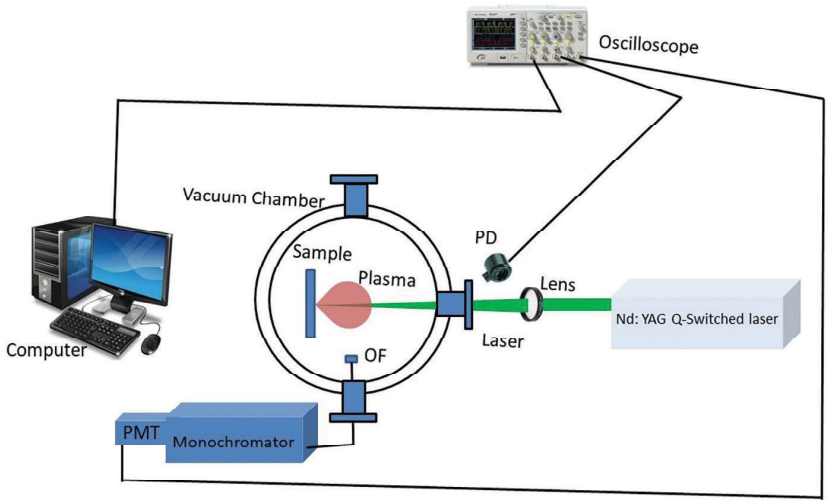

Fig. 4. Typical setup for examining the temporal evolution of plasma.

Table 2: List of important relations for Plasma Characterisation

Relations	
Boltzmann plot relation for finding electron temperature. [68]	$\ln\left(\frac{I_{mn}\lambda_{mn}}{A_{mn}g_m}\right) = \ln\left(\frac{n_n hc}{Z(T_e)}\right) - \left(\frac{E_m}{k_B T_e}\right)$

FWHM of Stark broadened line profile.[65]	$\Delta\lambda_{1/2} = 2w\left(\frac{n_e}{10^{16}}\right) + 3.5A\left(\frac{n_e}{10^{16}}\right)^{1/4} \times \left(1 - 1.2N_D^{-1/3}\right) w\left(\frac{n_e}{10^{16}}\right)$
FWHM of Stark broadened line profile after neglecting ion-impact term. Electron density can be determined from this relation.[68]	$\Delta\lambda_{1/2} = 2w\left(\frac{n_e}{10^{16}}\right)$
The experimental spectral line width ($\Delta\lambda_{1/2}$) can be corrected using this equation.[69]	$\Delta\lambda_{1/2} = \left(\left(w_g\right)^2 + \left(w_L^{\,2}/2\right)\right)^{1/2} + w_L/2$
Local thermodynamic equilibrium (LTE): McWhiter's criterion.[68]	$n_e \geq 1.6\times10^{12} T_e^{\frac{1}{2}} (\Delta E_{nm})^3$
Quantum mechanically corrected LTE condition.[70]	$n_e > \frac{2.55\times10^{11}}{\langle\bar{g}\rangle} T^{1/2} (\Delta E_{nm})^3$
For plasma to be strictly in LTE, these relations should be satisfied along with McWhiter's relation.[59]	$\frac{n_e(t+\tau_{rel}) - n_e(t)}{n_e(t)} < 1$ and $\frac{T_e(t+\tau_{rel}) - T_e(t)}{T_e(t)} < 1$
Relaxation time.[59]	$\tau_{rel} = \frac{6.3\times10^4}{\langle\bar{g}\rangle f_{mn} n_e} \Delta E_{nm} (kT_e)^{1/2} \exp(\Delta E_{nm}/kT_e)$
Excitation rate coefficient.[59]	$\langle\sigma_{nm} v_e\rangle = 1.60\times10^{-5} \frac{f_{nm}\langle\bar{g}\rangle}{\Delta E_{mn}(kT_e)^{1/2}} e^{-\Delta E_{mn}/kT_e} cm^3 s^{-1}$

The relation connecting the thermal diffusion length, thermal diffusivity of the material (D), and laser pulse width (τ) is [71] $L_{th} = (2D\tau)^{1/2}$. If the absorption depth α^{-1} << thermal diffusion length, then the energy absorbed within the time of pulse-width is utilised to heat the volume ($L_{th}\pi w^2$), where w is the radius of the laser spot on the surface. The absorbed laser energy is equal to the $(1-R)I\tau$. R is the wavelength-dependent reflectivity of the sample, and I is the intensity of the laser. Therefore, the temperature rise (ΔT) can be obtained from the relation $(1-R)I\tau = \rho C_V L_{th} \Delta T$. However, if the α^{-1} > thermal diffusion length, then the absorbed laser energy induces a surface temperature profile along the depth (z) and is given by [72] $(1-R)\alpha I e^{-\alpha z}\tau = \rho C_V L_{th} \Delta T$. When the absorbed energy per unit volume exceeds the latent heat of vaporisation, the mass in the volume ($L_{th}\pi w^2$) gets vaporised. The

vaporisation process causes the material removal, and the vaporisation rate is [73] $u = \frac{\alpha}{\rho(2\pi RT)^{1/2}}\left(P_{vap} - P_a\right)$, P_{vap} and P_0 denote the saturated vapour pressure and surrounding pressure. $\acute{a}$ is the correction factor for the backscattered vaporised atoms. The mechanical material removal process is known as melt ejection. During the nanosecond LA process, a molten layer forms on the laser-created crater surface. The LPP's recoil pressure exerts a thrust on the molten layer, causing the molten mass to eject. The recoil pressure of the LPP is approximately equal to half of the vapour pressure, which is given by the Clausius-Clapeyron equation [74], $P_{vap}\left(T_S\right) = P_a \exp\left[\frac{\Delta H\left(T_s - T_b\right)}{RT_sT_b}\right]$, where T_{b} and ΔH are, respectively, the vaporisation temperature and the latent heat of vaporisation. The fundamental issue of nanosecond LA is the shielding effect of LPP. Plasma absorbs laser energy, which reduces the laser-surface coupling. The plasma shielding effect occurs when the pulse width exceeds the plasma formation time. Plasma absorbs laser energy, which reduces the laser-target coupling. The plasma shielding effect occurs if the pulse width is longer than the plasma formation time. The magnetic field is successfully used to reduce plasma shielding by reducing the debris in the plasma. Researchers have investigated the LA in a magnetic field and observed a significant improvement in LA efficiency [23,26,32,75]. The phenomenon was ascribed to plasma magnetic confinement, resulting in enhanced plasma-target interaction and ejection of molten material. A magnetic field intensifies the recoil pressure of plasma, leading to a higher melt ejection rate than that without a magnetic field. Another possibility is the occurrence of magneto-absorption effects. When researchers applied a magnetic field to laser micromachining, they observed a high rate of material removal and an improvement in the depth-to-diameter ratio [18,34].

ii. Plasma Plume Confinement

LIBS is referred to as a flexible method for the elemental analysis of materials [76]. It has many benefits over other spectroscopic techniques, including application to various sample types (solid, liquid, gas), multi-element analysis, and the absence of sample preparation requirements [1,77]. This is an atomic emission spectroscopy, wherein

a high-intensity laser beam concentrates on a substance to generate LPP. LPP emits radiation of a wide frequency range. The plasma emission is recorded and analysed to understand the compositions of the target. The typical LIBS experimental setups are discussed in section 3. The major issue with this technique is its low sensitivity. Many research groups studied LIBS [78,79] to improve its sensitivity. Methods for improving the signal of LIBS include purging ambient gas, oblique laser radiation incidence, double pulse excitation, and laser radiation polarisation [5,10,51,59]. In recent years, the magnetic field has been engaged to increase the optical emission intensity of LPP. Investigation on LPP showed the improvement of the signal of LIBS [5,8,9,11,12,32,42] by magnetic confinement of plasma. It enhanced the emission from plasma irrespective of atomic or ionic transitions [12,32,80–82]. However, their improvement factors are varied for different materials. The Lorentz force segregates the electrons and ions when LPP flows within a magnetic field, resulting in an electric field $\vec{E}$ perpendicular to the applied magnetic field $\vec{B}$. Consequently, the plasma is subjected to $\vec{E}\times\vec{B}$ drift in $\vec{B}$. The induced current density $\vec{J}$ in plasma can be obtained by generalized Ohm's law [83] $\vec{E}+\left(\vec{V}\times\vec{B}\right)=\vec{J}/\sigma_0+\left(\vec{J}\times\vec{B}\right)/n_e e$ where $\vec{V}$, σ_0, e and n_e are, respectively, plasma expansion velocity, electrical conductivity, charge and density of the electron. The LPP is decelerated by the force density $\vec{J}\times\vec{B}$ and confined to a smaller volume, leading to a rise in density. The velocity (v_B) of decelerated LPP is given by [5,14,45,84].

$$v_B=\left(1-\frac{1}{\beta}\right)^{1/2} v_0 \tag{1}$$

$$\beta=\frac{2n_e kT_e}{B^2/\mu_0} \tag{2}$$

where v_0 is the plasma velocity without a magnetic field and β is equal to the ratio of the thermal pressure of LPP to the magnetic pressure. Plasma confinement occurs when β is less than 1. The magnetic plasma confinement increases both its electron temperature and density, hence enhancing the rate of collisional excitation and recombination. The amplification in optical emission is caused by the rise in collision-induced atomic excitation and recombination processes. Plasma, being a highly conductive medium, exhibits diamagnetism, which

expels magnetic flux. The plasma expands diamagnetically until the magnetic energy, excluded from its volume, equals the total kinetic energy of the plasma plume. The plasma slows down considerably at the diamagnetic cavity radius (the stopping radius). By equating the work required for the plasma to expel the $\vec{B}$ from LPP volume with its total energy, one can calculate this radius [59,85]. Consequently, the conservation of energy yields this radius and is given by [67,86]

$$R_0 = \left(\frac{3\mu_0 E_{La}}{\pi B^2} \right)^{1/3} \tag{3}$$

where E_{La} is the laser energy absorbed in the target. However, if the plasma evolves in a region where the magnetic field and the ambient gas exist, it experiences both gas and magnetic pressure. To account for the effect of air pressure, Singh et al. [4] incorporated air pressure in equation (2) and became

$$E_{La} = \tfrac{1}{2} m v^2 + \left(\frac{B^2}{2\mu_0} \right) V + \int P_{air} dV$$

$$R_0 = \left(\frac{3E_L}{4\pi} \frac{1}{(P_{air} + B^2 / 2\mu_0)} \right)^{1/3} \tag{4}$$

The evolution of LPP in an environment of both a magnetic field and an ambient gas has been examined using fast-gated CCD and ICCD cameras [2,3,25,87,88]. They showed that the laser plasma significantly decelerated around the stopping radius. However, the instability of LPP prevents it from stopping entirely.

iii. Instability of LPP

LPP with a magnetic field generally produces instabilities. The two types of instabilities, which are often seen in laser plasma, are Rayleigh-Taylor (RT) and Kelvin-Helmholtz (KH) instabilities [15,59]. The interface remains stable when the dense fluid pushes the less dense fluid. Rayleigh-Taylor instability arises at the boundary between two fluids of different densities when the less dense fluid pushes the denser fluid. It is a fingering instability of the interface. It can be illustrated in the water-air interface. The thick layer of water plastered on the ceiling of a room will fall. It is not because of the

insufficient air pressure to support the water layer. It falls due to RT instability [89]. When a laser plasma flows in an ambient gas, RT instability may occur at their interface depending on the experimental conditions. For a plasma of density (ρ_1) expanding in an ambient gas of density (ρ_2) , the generation of RT instability at the plasma-ambient boundary is determined by [90,91]

$$\omega^2 = -kg\frac{(\rho_1 - \rho_2)}{(\rho_1 + \rho_2)} = -kg\alpha \tag{5}$$

where g is the acceleration of the interface between the two fluids. If $\omega^2 > 0$ the plasma-ambient boundary is stable and if $\omega^2 < 0$ the fingering instability at the boundary grows exponentially. The instability growth time is $\tau = (kg\alpha)^{1/2}$. The RT instability of magnetised plasma occurs when it is supported against the gravitational field by magnetic pressure [15]. Another instability of magnetohydrodynamics is KH instability. This instability arises at the contact line of two fluids of different densities when the velocity of one fluid exceeds the critical velocity [21]. If σ is the fluid's surface tension, then the critical velocity [21] is $v_c \approx \left(\frac{4\sigma g\rho_l}{\rho_v{}^2}\right)^{1/4}$.

iv. Enhancement of Laser-Induced Breakdown Spectroscopy Signal

Researchers have investigated LPP without and with a magnetic field, demonstrating the enhancement of both atomic and ionic transitions. Table 3 lists the types of samples, the intensity of the magnetic field, and the enhancement factors for previous studies. The magnetic confinement of LPP is responsible for this improvement in atomic and ionic line intensities. Rai et al. [14] established a model relating the total plasma emission with the density and volume of LPP. The model elucidates how the confinement of LPP causes intensity enhancement. According to Rai et al. [14] , the LPP's total amount of radiation is directly proportional to its volume and the square of the density. Using the following relation [14], one can determine the ratio of intensities when a magnetic field is switched on or off.

$$\frac{I_B}{I_0} = \left(\frac{v_0 t_0}{v_B t_B}\right)^3 \tag{6}$$

Table 3 Recent studies on magnetically confined plasma for emission enhancement

Sample	Magnetic field	Enhancement of optical emission	Reference
Al alloy and aqueous solution of Mn, Mg, Ti, and Cr	0.5 T	2 times enhancement for solid sample and 1.5 times for liquid sample.	[14,93,94]
Zn	0.1-0.5T	Enhancement was observed in low laser energy.	[94]
Al	0.5 - 0.9 T	Both atomic and ionic lines were enhanced.	[2,7,11,36, 95,96]
Co	0.8 T	22 times in emission of Co. Reduction in intensity was observed in Co lines.	[9,11]
Cr	0.8 T	24 times enhancement in the emission of Cr.	[9]
Cu	0.1 T – 0.67 T	Enhancement was observed both in atomic and ionic lines.	[4,5,10,11, 32,43,51, 59,94]
Li	0.04 T -1.1 T	Enhancement was observed both in atomic and ionic lines.	[42,97,98]
V_2O_5	0.45 T	Enhancement was observed	[44]
ZrO_2		Enhancement was observed	[99]
Soil sample	0.3 T-0.7 T	8 times enhancement was observed. Enhancement of the detection limit of Cu and PB was observed	[100,101]
W	1.1 T	Atomic and ionic line intensity were enhanced.	[55]
Pd	0.12	Both the atomic and ionic lines were enhanced by 3-4 times.	[46]
Ge	0.45 T	Reduction in intensity	[81]
Sn	0.6 T	2 times in atomic and ionic lines	[62]
Graphite	0.5 T	Enhancement was observed.	[62]

t_0 and t_B are the emission times without and with a magnetic field, respectively. Using equation (1), equation (6) can be simplified as

$$\frac{I_B}{I_0} = \left(1 - \frac{1}{\beta}\right)^{-3/2} \left(\frac{t_0}{t_B}\right)^3 \tag{7}$$

Equation (7) shows that the optical emission enhancement mainly depends on β and the time of emissions. When the β is low, the improvement of emission is possible. This demonstrates that emission gets enhanced when the magnetic pressure dominates the plasma pressure. When the β is low, i.e., plasma is confined, the plasma emission gets enhanced. It is attributed to the rise in the rate of radiative recombination and electron impact-atomic transition. This can be comprehended by examining the rate of atomic transition resulting from the electron-atom collision, which is given by [92] $R_{nm} = n_e n \langle \sigma_{nm} v_e \rangle$, where n, σ_{nm}, and v_e are the density of atoms, the cross-section of electron-atom collision, and velocity of the electron, respectively. The rate coefficient, $\langle \sigma_{nm} v_e \rangle$ is estimated using the relation [92]

$$\langle \sigma_{nm} v_e \rangle = 1.60 \times 10^{-5} \frac{f_{nm} \langle \bar{g} \rangle}{\Delta E_{mn} (kT_e)^{1/2}} e^{-\Delta E_{mn}/kT_e} cm^3 s^{-1}, \tag{8}$$

where $\langle \bar{g} \rangle$ is the average Gaunt factor, f_{nm} is the absorption oscillator strength, and ΔE_{mn} is the energy difference between the states m and n, respectively. Confining the plasma increases the electron density, which raises the electron-atom or electron-ion collisional excitation rate. After the laser had terminated, the gain in LPP optical emission intensity from solid and liquid samples was most noticeable. Because the plasma thermal pressure is much higher than the magnetic pressure during the early time of plasma expansion, the role of the magnetic field is not significant., i.e., $\beta > 1$, during the early time of plasma expansion, the plasma is not confined by a magnetic field.

At early delay times before $2\,\mu s$, when the plasma temperature was very high, there was no enhancement [5,14]. We found that the enhancement of line emission significantly increased at gate delay times $2\,\mu s$ to $30\,\mu s$, with an enhancement factor of 1.5 [14]. When plasma magnetic confinement worked well, there was more radiative recombination, which led to a rise in line emission intensity at a later time in plasma evolution. The intensity of optical emission of LPP from solid and liquid samples was found to be increased initially and

then decreased gradually with laser pulse energy. At higher laser energy, the intensity of optical emission reached saturation. In the absence of a magnetic field, the onset of optical emission saturation occurred at laser energy 225 mJ [5,14]. The saturation in optical emission was attributed to self-absorption, which arose due to the increase in density of the plasma. The onset of saturation was found to be observed at a comparatively lower energy in the presence of the magnetic field. The enhancement of optical emission was observed below 225 mJ laser energy, and the intensity in the presence of a magnetic field was found to be lower than that without a magnetic field when the laser energy was above 225 mJ [93].

v. Electron Density and Temperature

The spectroscopic technique called LIBS is capable of gathering and examining the radiation emitted by plasma. During the later phase of plasma expansion, atomic spectral transition lines that represent the unique characteristics of the sample components are released. These measurements offer both quantitative and qualitative data regarding the composition of the material sample [1]. However, if there is any component of a trace amount in the sample, the transition line intensities are poor. This may make determining the presence of this component uncertain. The magnetic field can be used to enhance the intensity of the LIBS signal [9,11]. When the magnetic field confines laser plasma, its temperature and density increase significantly [6,12,80,87]. Increasing temperature and plasma density increases the recombination and excitation rate and, hence, the intensity [14].

5. Conclusion

LA has a wide range of applications and is studied well by many research groups for different aspects. The comparative studies on LA in the absence and presence of magnetic fields are rarely available in the literature. LA in a magnetic field involves a variety of physical processes. Understanding these processes can aid in optimising the laser parameters to improve thin film quality, control nanoparticle size, achieve precise and smooth material cutting or drilling, perform laser surgery, and enhance the LIBS signal, among other benefits. It may also be helpful to design the portable LIBS setup to analyse the soil and other materials outside the laboratory.

Nomenclature

R_0	Stopping radius
β	The ratio of plasma pressure to the magnetic pressure
B	Magnetic field
E_{la}	Absorbed laser energy by the target
v_B	Velocity of plasma in the presence of magnetic field.
V_0	Velocity of plasma in the absence of magnetic field.
T_S	Target surface temperature
n_e	Electron density
T_e	Electron temperature
I_B	Intensity of optical emission in the presence of magnetic field
I_0	Intensity of optical emission in the absence of magnetic field

Author's contribution

Khwairakpam Shantakumar Singh: Conceptualization and Literature review, Writing-Original draft, review and editing

Funding

This review work received no grants from any funding agency.

Conflict of Interest

The author declares no conflict of interest.

References

[1] J. P. Singh, S. N. Thakur, Laser Induced Breakdown Spectroscopy, Elsevier, Amsterdam, 2007.

[2] S. S. Harilal, M. S. Tillack, B. O'Shay, C. V Bindhu, F. Najmabadi, Confinement and dynamics of laser-produced plasma expanding across a transverse magnetic field, Phys. Rev. E. 69 (2004) 26413 (1–11).

[3] N. Behera, R. K. Singh, A. Kumar, Confinement and re-expansion of laser induced plasma in transverse magnetic field: Dynamical behaviour and geometrical aspect of expanding plume, Phys. Lett. A. 379 (2015) 2215–2220.

[4] K.S. Singh, A.K. Sharma, Spatially resolved behaviour of laser-produced copper plasma along expansion direction in the presence of static uniform magnetic field, Phys. Plasmas. 23 (2016) 122104. https://doi.org/10.1063/1.4969080.

[5] Y. Li, C.H. Hu, H.Z. Zhang, Z.K. Jiang, Z.S. Li, Optical emission enhancement of laser-produced copper plasma under a steady magnetic field, Appl. Opt. 48 (2009) B105–B110.

[6] V.N. Rai, Theoretical aspect of enhancement and saturation in emission from laser produced plasma, Laser Part. Beams. 30 (2012) 621–631.

[7] A. Hussain, X. Gao, Z. Hao, J. Lin, Combined effects of double pulses and magnetic field on emission enhancement of laser-induced breakdown spectroscopy from aluminum plasma, Optik (Stuttg). 127 (2016) 10024–10030. https://doi.org/10.1016/j.ijleo.2016.07.047.

[8] M. Akhtar, A. Jabbar, N. Ahmed, S. Mehmood, Z.A. Umar, R. Ahmed, M.A. Baig, Magnetic field-induced signal enhancement in laser-produced lead plasma, Laser Part. Beams. 37 (2019) 67–78. https://doi.org/10.1017/S0263034619000144.

[9] L.B. Guo, W. Hu, B.Y. Zhang, X.N. He, C.M. Li, Y.S. Zhou, Z.X. Cai, X.Y. Zeng, Y.F. Lu, Enhancement of optical emission from laser-induced plasmas by combined spatial and magnetic confinement, Opt. Express. 19 (2011) 14067–14075.

[10] K.S. Singh, A.K. Sharma, Time-integrated optical emission studies on laser-produced copper plasma in the presence of magnetic field in air ambient at atmospheric pressure, Appl. Phys. A Mater. Sci. Process. 123 (2017) 325. https://doi.org/10.1007/s00339-017-0953-y.

[11] X.K. Shen, Y.F. Lu, T. Gebre, H. Ling, Y.X. Han, Optical emission in magnetically confined laser-induced breakdown spectroscopy, J. Appl. Phys. 100 (2006) 053303(1–7).

[12] V.N. Rai, J.P. Singh, F.Y. Yueh, R.L. Cook, Study of optical emission from laser-produced plasma expanding across an external magnetic field, Laser Part. Beams. 21 (2003) 65–71. https://doi.org/Doi 10.1017/S0263034603211137.

[13] C. Pagano, S. Hafeez, J.G. Lunney, Influence of transverse magnetic field on expansion and spectral emission of laser produced plasma, J. Phys. D-Appl. Phys. 42 (2009) 155205 (1–7).

[14] V.N. Rai, A.K. Rai, F.Y. Yueh, J.P. Singh, Optical emission from laser-induced breakdown plasma of solid and liquid samples in the presence of a magnetic field, Appl. Opt. 42 (2003) 2085–2093.

[15] R.K.T. A. Neogi, 942 Instabilities in laser-produced carbon plasma expanding in a nonuniform magnetic field, Appl. Phys. B. 72 (2001) 231–235.

[16] K. Takahashi, T. Uchino, K. Ikegami, T. Sasaki, T. Kikuchi, N. Harada, Behavior of Laser Ablation Plasma during Transport in Multicusp Magnetic Field Using Different Targets for Laser Ion Source, in: Energy Procedia, Elsevier Ltd, 2017: pp. 354–358. https://doi.org/10.1016/j.egypro.2017.09.467.

[17] C. Ye, G.J. Cheng, S. Tao, B.X. Wu, Magnetic Field Effects on Laser Drilling, J. Manuf. Sci. Eng. Asme. 135 (2013) 061020(1–5).

[18] S. Wolff, I. Saxena, A preliminary study on the effect of external magnetic fields on Laser-Induced Plasma Micromachining (LIPMM), Manuf. Lett. 2 (2014) 54–59. https://doi.org/10.1016/j.mfglet.2014.02.003.

[19] M.H. Mohsin, R.A. Ismail, R.O. Mhadi, Preparation of nanostructured FeS2/Si heterojunction photodetector by laser ablation in water under effect of an external magnetic field, Appl. Phys. A. 127 (2021) 214. https://doi.org/10.1007 /s00339-021-04369-0.

[20] K.K. Kim, M. Roy, H. Kwon, J.K. Song, S.M. Park, Laser ablation dynamics in liquid phase: The effects of magnetic field and electrolyte, J. Appl. Phys. 117 (2015) 074302. https://doi.org/10.1063/1.4913253.

[21] K.S. Singh, A.K. Sharma, Melt ejection from copper target in air in the presence of magnetic field using nanosecond pulsed laser ablation, J. Vac. Sci. Technol. A Vacuum, Surfaces Film. 35 (2017) 031305. https://doi.org/10.1116/1.4979663.

[22] P.K. Pandey, S.L. Gupta, R.K. Thareja, Study of pulse width and magnetic field effect on laser ablated copper plasma in air, Phys. Plasmas. 22 (2015) 073301. https://doi.org/10.1063/1.4926528.

[23] K.S. Singh, A.K. Sharma, Effect of variation of magnetic field on laser ablation depth of copper and aluminum targets in air atmosphere, J. Appl. Phys. 119 (2016) 183301. https://doi.org/10.1063/1.4948950.

[24] O.R. Musaev, E.A. Sutter, J.M. Wrobel, M.B. Kruger, The effect of magnetic fields on the products of laser ablation, Appl. Phys. A. 122 (2016) 95 (1–5). https://doi.org/10.1007/s00339-016-9636-3.

[25] D.N. Patel, P.K. Pandey, R.K. Thareja, Brass plasmoid in external magnetic field at different air pressures, Phys. Plasmas. 20 (2013) 103503.

[26] H. Farrokhi, V. Gruzdev, H.Y. Zheng, R.S. Rawat, W. Zhou, Magneto-absorption effects in magnetic-field assisted laser ablation of silicon by UV nanosecond pulses, Appl. Phys. Lett. 108 (2016) 254103. https://doi.org/10.1063/1.4954708.

[27] H. Farrokhi, V. Gruzdev, H. Zheng, W. Zhou, Fundamental mechanisms of nanosecond-laser-ablation enhancement by an axial magnetic field, J. Opt. Soc. Am. B. 36 (2019) 1091. https://doi.org/10.1364/josab.36.001091.

[28] J. Maksimovic, S.H. Ng, T. Katkus, B.C.C. Cowie, S. Juodkazis, External Field-Controlled Ablation: Magnetic Field, Nanomaterials. 9 (2019) 1662. https://doi.org/10.3390/nano9121662.

[29] O.R. Musaev, E.A. Sutter, J.M. Wrobel, M.B. Kruger, The effect of magnetic fields on the products of laser ablation, Appl. Phys. A Mater. Sci. Process. 122 (2016) 1–5. https://doi.org/10.1007/s00339-016-9636-3.

[30] K.S. Singh, A.K. Sharma, Melt ejection from copper target in air in the presence of magnetic field using nanosecond pulsed laser ablation, J. Vac. Sci. Technol. A Vacuum, Surfaces, Film. 35 (2017) 031305. https://doi.org/10.1116/1.4979663.

[31] K.S. Singh, A.K. Sharma, Effect of variation of magnetic field on laser ablation depth of copper and aluminum targets in air atmosphere, J. Appl. Phys. 119 (2016) 183301. https://doi.org/10.1063/1.4948950.

[32] K.S. Singh, A. Khare, A.K. Sharma, Effect of uniform magnetic field on laser-produced Cu plasma and the deposited particles on the target surface, Laser Part. Beams. 35 (2017) 352. https://doi.org/10.1017/S0263034617000271.

[33] C.-C. Ho, G.-R. Tseng, Y.-J. Chang, J.-C. Hsu, C.-L. Kuo, Magnetic-field-assisted laser percussion drilling, Int. J. Adv. Manuf. Technol. 73 (2014) 329–340. https://doi.org/10.1007/s00170-014-5815-6.

[34] Y.J. Chang, C.L. Kuo, N.Y. Wang, Magnetic Assisted Laser Micromachining for Highly Reflective Metals, J. Laser Micro Nanoeng. 7 (2012) 254–259. https://doi.org/DOI 10.2961/j1mn.2012.03.0004.

[35] I. Saxena, S. Wolff, J. Cao, Unidirectional magnetic field assisted Laser Induced Plasma Micro-Machining, Manuf. Lett. 3 (2015) 1–4. https://doi.org/10.1016/J. MFGLET.2014.09.001.

[36] A. Hussain, H. Asghar, M. Tanveer, M. Zafar, Qura-Tul-Ain, Z. Nawaz, Spectral emission improvement by combining ambient pressures and magnetic field-deployment in laser-induced breakdown spectroscopy, Optik (Stuttg). 201 (2020). https://doi.org/10.1016/j.ijleo.2019.163340.

[37] Y. Wang, A. Chen, D. Zhang, Q. Wang, S. Li, Y. Jiang, M. Jin, Enhanced optical emission in laser-induced breakdown spectroscopy by combining femtosecond and nanosecond laser pulses, Phys. Plasmas. 27 (2020) 023507. https://doi.org/10.1063/1.5131772.

[38] V. Sivakumaran, A. Kumar, R.K. Singh, V. Prahlad, H.C. Joshi, Atomic Processes in Emission Characteristics of a Lithium Plasma Plume Formed by Double-Pulse Laser Ablation, Plasma Sci. Technol. 15 (2013) 204–208. https://doi.org/10.1088/1009-0630/15/3/02.

[39] R. Viskup, B. Praher, T. Linsmeyer, H. Scherndl, J.D. Pedarnig, J. Heitz, Influence of pulse-to-pulse delay for 532 nm double-pulse laser-induced breakdown spectroscopy of technical polymers, Spectrochim. Acta - Part B At. Spectrosc. 65 (2010) 935–942.

[40] P.K. Diwakar, S.S. Harilal, J.R. Freeman, A. Hassanein, 4 Role of laser pre-pulse wavelength and inter-pulse delay on signal enhancement in collinear double-pulse laser-induced breakdown spectroscopy, Spectrochim. Acta - Part B. 87 (2013) 65–73.

[41] Y. Li, D. Tian, Y. Ding, G. Yang, K. Liu, C. Wang, X. Han, A review of laser-induced breakdown spectroscopy signal enhancement, Appl. Spectrosc. Rev. 53 (2018). https://doi.org/10.1080/05704928.2017.1352509.

[42] H.C. Joshi, A. Kumar, R.K. Singh, V. Prahlad, Effect of a transverse magnetic field on the plume emission in laser-produced plasma: An atomic analysis, Spectrochim. Acta Part B. 65 (2010) 415–419.

[43] D.H. Xu, C. Song, S.Y. Zhao, X. Gao, J.Q. Lin, Magnetic Confinement Effect on Femtosecond Laser-induced Copper Plasma, Guangzi Xuebao/ Acta Photonica Sin. 47 (2018). https://doi.org/10.3788/gzxb20184708.0847012.

[44] S. Amin, S. Bashir, S. Anjum, M. Akram, A. Hayat, S. Waheed, H. Iftikhar, A. Dawood, K. Mahmood, Optical emission spectroscopy of magnetically confined laser induced vanadium pentoxide (V2O5) plasma, Phys. Plasmas. 24 (2017) 083112. https://doi.org/10.1063/1.4994067.

[45] P. Liu, R. Hai, D. Wu, Q. Xiao, L. Sun, H. Ding, The enhanced effect of optical emission from laser induced breakdown spectroscopy of an Al-Li Alloy in the presence of magnetic field confinement, in: Plasma Sci. Technol., Institute of Physics Publishing, 2015: pp. 687–692. https://doi.org/10.1088/1009-0630/17/8/13.

[46] S.A. Abbasi, Z. Aziz, T.M. Khan, D. Ali, T. ul Hassan, J. Iqbal, S.U.D. Khan, A. Ahmad, R. Khan, E.M. Khan, Enhancement of optical signal and characterizati- on of palladium plasma by magnetic field-assisted laser-induced breakdown spectroscopy, Optik (Stuttg). 224 (2020). https://doi.org/10.1016/j.ijleo.2020.16 5746.

[47] Y. Fu, Z. Hou, Z. Wang, Physical insights of cavity confinement enhancing effect in laser-induced breakdown spectroscopy, Opt. Express. 24 (2016). https://doi.org/10.1364/oe.24.003055.

[48] M.R. Khan, S.U. Haq, Q. Abbas, A. Nadeem, Magnetic field confined laser-induced plasma: Improvement in sensitivity and repeatability, Spectrochim. Acta Part B At. Spectrosc. 200 (2023) 106612. https://doi.org/10.1016/J.SAB.202 2.106612.

[49] J. Li, J. Wu, M. Shi, Y. Qiu, Y. Zhou, H. Sun, X. Guo, D. Wu, Y. Hang, H. Yang, X. Li, Synergy enhancement and signal uncertainty of magnetic-spatial confinement in fiber-optic laser-induced breakdown spectroscopy, J. Anal. At. Spectrom. 39 (2024) 1235–1247. https://doi.org/10.1039/D3JA00401E.

[50] L. Nagli, A. Prosnyakov, M. Gaft, Y. Raichlin, Effect of crater volume on laser-induced plasma lasers and Laser-Induced Breakdown Spectroscopy intensity, Spectrochim. Acta - Part B At. Spectrosc. 183 (2021). https://doi.org/10.1016/j.sab.2021.106246.

[51] K.S. Singh, A.K. Sharma, Effect of lens focusing distance on laser-produced copper plasma in air in the presence of static transverse magnetic field, Phys. Plasmas. 23 (2016) 123514. https://doi.org/10.1063/1.4971815.

[52] A. Kumar, R.K. Singh, J. Thomas, S. Sunil, Parametric study of expanding plasma plume formed by laser-blow-off of thin film using triple Langmuir probe, J. Appl. Phys. 106 (2009) 043306 (1–8).

[53] J. Kiefer, J. Kiefer, Simultaneous Application of Raman and Laser-Induced Breakdown Spectroscopy in the Gas Phase with a Single Laser and Detector, Appl. Spectrosc. Vol. 78, Issue 4, Pp. 438-441. 78 (2024) 438–441. https://doi.org/10.1177/00037028241227459.

[54] H.B. Andrews, M.Z. Martin, A.M. Wymore, U.C. Kalluri, Rapid in situ nutrient element distribution in plants and soils using laser-induced breakdown spectroscopy (LIBS), Plant Soil. 495 (2024) 3–12. https://doi.org/10.1007/S1110 4-023-05988-7/ METRICS.

[55] D. Wu, L. Sun, R. Hai, J. Liu, Y. Hao, X. Yu, C. Li, C. Feng, P. Liu, H. Ding, Influence of transverse magnetic field on plume dynamics and optical emission of nanosecond laser produced tungsten plasma in vacuum, Spectrochim. Acta - Part B At. Spectrosc. 169 (2020) 105882. https://doi.org/10.1016/j.sab.2020.1058 82.

[56] A. Mondal, R.K. Singh, V. Chaudhari, H.C. Joshi, Effect of magnetic field on the lateral interaction of plasma plumes, Phys. Plasmas. 27 (2020) 093109. https://doi.org/10.1063/5.0006647.

[57] W. Zhou, C. Zhang, Y. Liu, Y. Li, L. Jiang, L. Ren, X. Chu, Magnetic field assisted laser fabrication and electrical characterizations of metal dry Biolectrode with surface microstructures, Biomed. Microdevices. 21 (2019) 1–12. https://doi.org/10.1007/s10544-019-0422-9.

[58] A. Dawood, S. Bashir, N.A. Chishti, M.A. Khan, A. Hayat, Magnetic field effect on plasma parameters and surface modification of laser-irradiated Cu-alloy, Laser Part. Beams. 36 (2018) 261–275. https://doi.org/10.1017/S0263034618000 137.

[59] K.S. Singh, A.K. Sharma, Multi-structured temporal behavior of neutral copper transitions in laser-produced plasma in the presence of variable transverse static magnetic field, Phys. Plasmas. 23 (2016) 013304. https://doi.org/10.1063/1.4939883.

[60] A. Arshad, S. Bashir, A. Hayat, M. Akram, A. Khalid, N. Yaseen, Q.S. Ahmad, Effect of magnetic field on laser-induced breakdown spectroscopy of graphite plasma, Appl. Phys. B. 122 (2016) 63. https://doi.org/10.1007/s00340-016-6333-z.

[61] A. Neogi, V. Narayanan, R.K. Thareja, Optical emission studies of laser ablated carbon plasma in a curved magnetic field, Phys. Lett. A. 258 (1999) 135–140.

[62] H. Lan, X.B. Wang, H. Chen, D.L. Zuo, P.X. Lu, Influence of a magnetic field on laser-produced Sn plasma, Plasma Sources Sci. Technol. 24 (2015) 055012 (1–7).

[63] L. Godbert-Mouret, M. Koubiti, R. Stamm, K. Touati, B. Felts, H. Capes, Y. Corre, R. Guirlet, C. De Michelis, 986 Spectroscopy of magnetized plasmas, J. Quant. Spectrosc. Radiat. Transf. 71 (2001) 365–372. https://doi.org/Doi 10.1016/S0022-4073(01)00082-6.

[64] D.N. Stratis, K.L. Eland, S.M. Angel, 987 Effect of pulse delay time on a pre-ablation dual-pulse LIBS plasma, Appl. Spectrosc. 55 (2001) 1297–1303.

[65] M. Hanif, M. Salik, M.A. Baig, Quantitative studies of copper plasma using laser induced breakdown spectroscopy, Opt. Lasers Eng. 49 (2011) 1456–1461.

[66] R.K.T. A.K. Sharma, 988 Plume dynamics of laser-produced aluminum plasma in ambient nitrogen, Appl. Surf. Sci. 243 (2005) 68–75.

[67] M.S. Raju, R.K. Singh, P. Gopinath, A. Kumar, Influence of magnetic field on laser-produced barium plasmas: Spectral and dynamic behaviour of neutral and ionic species, J. Appl. Phys. 116 (2014) 153301 (1–11).

[68] H.R. Griem, 990 Plasma Spectroscopy, McGraw Hill Book Company, USA, 1964.

[69] W.Lochte-Holtgreven, 991 Plasma Diagnostics, AIP Press, USA, 1995.

[70] H.R. Griem, 992 Validity of Local Thermal Equilibrium in Plasma Spectroscopy, Phys. Rev. 131 (1963) 1170–1176.

[71] D.N. Patel, P.K. Pandey, R.K. Thareja, Stoichiometry of laser ablated brass nanoparticles in water and air, Appl. Opt. 52 (2013) 7592–7601.

[72] S. Amoruso, R. Bruzzese, N. Spinelli, R. Velotta, Characterization of laser-ablation plasmas, J. Phys. B At. Mol. Opt. Phys. 32 (1999) R131. https://doi.org/10.1088/0953-4075/32/14/201.

[73] F.P. Mezzapesa, L.L. Columbo, M. Brambilla, M. Dabbicco, A. Ancona, T. Sibillano, G. Scamarcio, Laser ablation dynamics in metals: The thermal regime, Appl. Phys. Lett. 101 (2012) 011103. https://doi.org/10.1063/1.4732507.

[74] A. Bogaerts, Z. Chen, R. Gijbels, A. Vertes, Laser ablation for analytical sampling: what can we learn from modeling?, Spectrochim. Acta Part B At. Spectrosc. 58 (2003) 1867–1893. https://doi.org/10.1016/j.sab.2003.08.004.

[75] C.C. Ho, G.R. Tseng, Y.J. Chang, J.C. Hsu, C.L. Kuo, 963 Magnetic-field-assisted laser percussion drilling, Int. J. Adv. Manuf. Technol. 73 (2014) 329–340.

[76] A. De Giacomo, M. Dell'Aglio, O. De Pascale, R. Gaudiuso, A. Santagata, R. Teghil, 6 Laser Induced Breakdown Spectroscopy methodology for the analysis of copper-based-alloys used in ancient artworks, Spectrochim. Acta Part B. 63 (2008) 585–590. https://doi.org/10.1016/j.sab.2008.03.006.

[77] C. Pasquini, J. Cortez, L.M.C. Silva, F.B. Gonzaga, 5 Laser induced breakdown spectroscopy, J. Braz. Chem. Soc. 18 (2007) 463–512.

[78] G. Shukla, A. Khare, Spectroscopic studies of laser ablated ZnO plasma and correlation with pulsed laser deposited ZnO thin film properties, Laser Part. Beams. 28 (2010) 149. https://doi.org/10.1017/S0263034610000029.

[79] E. Schwarz, S. Gross, B. Fischer, I. Muri, J. Tauer, H. Kofler, E. Wintner, 965 Laser-induced optical breakdown applied for laser spark ignition, Laser Part. Beams. 28 (2010) 109 119. https://doi.org/10.1017/S0263034609990668.

[80] A. Roy, S.S. Harilal, S.M. Hassan, A. Endo, T. Mocek, A. Hassanein, 967 Collimation of laser-produced plasmas using axial magnetic field, Laser Part. Beams. 33 (2015) 175–182. https://doi.org/10.1017/S0263034615000075.

[81] H. Iftikhar, S. Bashir, A. Dawood, M. Akram, A. Hayat, K. Mahmood, A. Zaheer, S. Amin, F. Murtaza, Magnetic field effect on laser-induced breakdown spectroscopy and surface modifications of germanium at various fluences, Laser

Part. Beams. 35 (2017) 159–169. https://doi.org/10.1017/S0263034617000039.

[82] V.N. Rai, M. Shukla, H.C. Pant, 969 Some studies on picosecond laser produced plasma expanding across a uniform external magnetic field, Laser Part. Beams. 16 (2009) 431–443.

[83] J.A. Bittencourt, 970 Fundamentals of Plasma Physics, Springer, New York, 2004.

[84] A. Hussain, Q. Li, Z. Hao, X. Gao, J. Lin, The effect of an external magnetic field on the plume expansion dynamics of laser-induced aluminum plasma, in: Plasma Sci. Technol., Institute of Physics Publishing, 2015: pp. 693–698. https://doi.org/10.1088/1009-0630/17/8/14.

[85] M.S. Raju, R.K. Singh, A. Kumar, P. Gopinath, Diamagnetic cavitization of laser-produced barium plasma in transverse magnetic field, Opt. Lett. 40 (2015) 2185–2188.

[86] C. Pagano, S. Hafeez, J.G. Lunney, Influence of transverse magnetic field on expansion and spectral emission of laser produced plasma, J. Phys. D. Appl. Phys. 42 (2009). https://doi.org/10.1088/0022-3727/42/15/155205.

[87] A. Kumar, S. George, R.K. Singh, H. Joshi, V.P.N. Nampoori, Image analysis of expanding laser-produced lithium plasma plume in variable transverse magnetic field, Laser Part. Beams. 29 (2011) 241–247. https://doi.org/Doi 10.1017/S0263034611000218.

[88] P.K. Pandey, R.K. Thareja, Plume dynamics and cluster formation in laser-ablated copper plasma in a magnetic field, J. Appl. Phys. 109 (2011) 074901(1–9).

[89] D.H. Sharp, An overview of Rayleigh-Taylor instability, Phys. D Nonlinear Phenom. 12 (1984) 3–18. https://doi.org/10.1016/0167-2789(84)90510-4.

[90] A.K. Sharma, R.K. Thareja, Anisotropic emission in laser-produced aluminum plasma in ambient nitrogen, Appl. Surf. Sci. 253 (2007) 3113–3121. https://doi.org/10.1016/j.apsusc.2006.07.014.

[91] R.K. THAREJA, A.K. SHARMA, Reactive pulsed laser ablation: Plasma studies, Laser Part. Beams. 24 (2006) 311–320. https://doi.org/10.1017/S0263034606060484.

[92] J.D. Hey, Criteria for local thermal equilibrium in non-hydrogenic plasmas, J. Quant. Spectrosc. Radiat. Transf. 16 (1976) 69–75.

[93] V.N. Rai, H. Zhang, F.Y. Yueh, J.P. Singh, A. Kumar, Effect of steady magnetic field on laser-induced breakdown spectroscopy., Appl. Opt. 42 (2003) 3662–3669.

[94] D.H. Kim, Y.H. Kihm, S.J. Choi, J.J. Choi, J.J. Yoh, The application of magnetic field at low pressure for optimal laser-induced plasma spectroscopy, Spectrochim. Acta - Part B At. Spectrosc. 110 (2015) 7–12. https://doi.org/10.1016/j.sab.2015.05.006.

[95] A. Hussain, H. Asghar, T. Iqbal, M. Ishfaq, R.M. Shahbaz, Q. Riaz, Improving the spectral intensity of aluminum plasma by applied-magnetic field in laser-induced breakdown spectroscopy, Optik (Stuttg). 251 (2022). https://doi.org/10.1016/j.ijleo.2021.168220.

[96] N.A. Chishti, S. Bashir, A. Dawood, M.A. Khan, Laser-induced breakdown spectroscopy of aluminum plasma in the absence and presence of magnetic field, Appl. Opt. 58 (2019). https://doi.org/10.1364/ao.58.001110.

[97] A. Kumar, R.K. Singh, H. Joshi, Effect of transverse magnetic field on the laser-blow-off plasma plume emission in the presence of ambient gas, Spectrochim. Acta Part B. 66 (2011) 444–450.

[98] P. Liu, D. Wu, L. Sun, R. Hai, J. Liu, H. Ding, Magnetic field selective enhancement of Li I lines comparing Li II line in laser ablated lithium plasma at 10− 2 mbar air ambient gas, Spectrochim. Acta - Part B At. Spectrosc. 137 (2017). https://doi.org/10.1016/j.sab.2017.09.004.

[99] S. Waheed, S. Bashir, A. Dawood, S. Anjum, M. Akram, A. Hayat, S. Amin, A. Zaheer, *Effect of magnetic field on laser induced breakdown spectroscopy of zirconium dioxide (ZrO2) plasma, Optik (Stuttg). 140 (2017). https://doi.org/10.1016/j.ijleo.2017.04.046.

[100] M. Akhtar, A. Jabbar, N. Ahmed, S. Mahmood, Z.A. Umar, R. Ahmed, M.A. Baig, *Analysis of lead and copper in soil samples by laser-induced breakdown spectroscopy under external magnetic field, Appl. Phys. B Lasers Opt. 125 (2019). https://doi.org/10.1007/s00340-019-7225-9.